Hindawi
Advances in Materials Science and Engineering
Volume 2020, Article ID 5602163, 9 pages
https://doi.org/10.1155/2020/5602163

Research Article

Effect of Drying-Wetting Cycles on Engineering Properties of Expansive Soils Modified by Industrial Wastes

Chengfu Chu,[1] Meihuang Zhan,[1] Qi Feng,[1] Dong Li,[1] Long Xu,[1] Fusheng Zha,[1] and Yongfeng Deng[2]

[1]*Hefei University of Technology, School of Resources and Environmental Engineering, Hefei 230009, China*
[2]*Southeast University, School of Transportation, Nanjing 211189, China*

Correspondence should be addressed to Qi Feng; qifeng@hfut.edu.cn

Received 17 August 2020; Revised 19 October 2020; Accepted 26 November 2020; Published 8 December 2020

Academic Editor: Akbar Heidarzadeh

The swelling properties of expansive soils can be reduced by the addition of modifiers. Nevertheless, the performance deterioration after modification occurs when weathering for a long term. Therefore, in this study, the effect of drying-wetting cycles on swelling behaviour and compressibility of modified expansive soils with the iron tailing sand and calcium carbide slag has been investigated. The swelling potential initially increases and subsequently decreases with the increasing number of cycles, reaches the peak at the seventh cycle, and tends to equilibrium after the tenth cycle. These results show that drying-wetting cycles will destroy the soil structure. The compressibility of modified expansive soils increases with the drying-wetting cycles, where an empirical formula between compressibility and the cycle number was established. Microstructural analysis is performed using mercury intrusion porosimetry (MIP) and scanning electron microscopy (SEM). The results of microstructural analysis show a tendency of degradation process.

1. Introduction

Expansive soils are highly plastic soils and are mainly composed of hydrophilic clay minerals (i.e., montmorillonite group minerals). The behaviour of expansive soils changes with the water mass, i.e., expanding when absorbing water and shrinking when discharging water [1, 2]. The long-term evolution in climate and hydrological conditions will cause progressive alteration in deformation and strength, leading to the degradation of geo-based structures, including the highway, railway, slope, and foundation, and also causing a significant financial loss annually in the world [3–5].

Many improvement technologies have been proposed and applied in engineering practices, such as replacement, compaction, moisture control, chemical modification, and thermodynamics methods. Chemical additives such as cement, lime, and fly ash have been confirmed to effectively change the plasticity and swelling characteristics of the expansive soils [6–9]. Despite that cement and lime have been extensively used as they are cost effective, many industrial wastes, such as recycled fiber, glass, iron tailing sand, and carbide slag, have been regarded as the substitution of traditional modifiers for environmental protection and economic benefits [10–14]. Iron tailing sand and calcium carbide slag are the byproducts of iron mines and calcium carbide industries, respectively [15, 16], which bring serious environmental problems when disposing these wastes. Calcium carbide slag with high $Ca(OH)_2$ content may be a sustainable agent to substitute lime and cement when modifying expansive soil. Iron tailing sand composes of the fine and stable fraction, which could be used to optimize the particle size distribution [17, 18], the swelling pressure [19], and the shear strength [20] of expansive soil. Therefore, it is applicable to recycle these wastes as expansive soil modifiers.

Previous studies highlight that the stabilization of modified expansive soils depend on the type and content of modifier, curing period, temperature, and moisture control. Note that stabilization quality in working condition should be focused, especially in the alternate region between rainy and dry seasons. This alternation will weaken the stabilization quality and then lead to the engineering problems (deformation and cracks of geo-based structures). The beneficial effects of expansive soils modified by lime are partially lost after several drying-wetting cycles [21–25]. These results showed that irreversible damage of the improved geo-based structures could be triggered after experiencing the drying-wetting cycles [26–28]. In addition, for the geo-based structures (i.e., foundation and roadbed), the compressibility is another concentration for the long-term stability and safety [29–32].

In this study, the effects of drying-wetting cycles on the free swelling ratio, the swelling pressure, and the compressibility of expansive soils improved by the iron tailing sand and calcium carbide slag were explored. Furthermore, microstructure was investigated by the mercury intrusion porosimeter (MIP) and scanning electron microscope (SEM) tests as well to clarify the internal mechanism.

2. Materials and Methods

2.1. Materials. The expansive soil used in this study was sampled from Hefei, the central part of Anhui province, China. The basic physical properties of the soil are summarized in Table 1. Swelling potential was classified as "weak" according to the previous research studies [33]. Its maximum dry density of 1.84 g/cm^3 and the optimum water content of 16.6% are identified by the compaction test [34]. The particle size distribution was determined by the hydrometer analysis obeying ASTM D421-85 [35], and the clay fraction of the sample after drying-wetting cycles was also measured. The iron tailing sand (hereinafter abbreviated as ITS) and calcium carbide slag (hereinafter abbreviated as CCS) were both sampled in Anhui, China. The composition of the iron tailing sand was mainly primary minerals with stable structure, including quartz and feldspar. The main chemical composition of calcium carbide slag is shown in Table 2. The main chemical composition and the particle size distribution of iron tailing sand are shown in Tables 3 and 4, respectively.

During sample preparation, the expansive soil and the industrial wastes were oven-dried at 105°C for 36 h and then ground into powders and sieved through a 0.5 mm sieve. According to Ye et al. [13], the iron tailing sand content of 30% can effectively inhibit swelling and achieve the requirements for engineering construction. Therefore, the soil mixed with iron tailing sand at a mass proportion (a_{ITS}) of 30% and with calcium carbide slag at a mass proportion (a_{CCS}) of 6%, 8%, 10%, 12%, and 14% was designed respectively. Hereinafter, the water content of mixtures was adjusted to the optimal water content depending on a_{ITS} and a_{CCS} (Table 4). After 24 h of curing period in an airtight container, the mixtures were statically compacted in a mould with 20 mm height and 61.8 mm diameter to reach the maximum dry density (Table 5). Finally, the prepared samples were cured under standard curing conditions (temperature of 20°C and relative humidity of 95%) for 28 days.

2.2. Drying-Wetting Cycle Tests. Cycled drying-wetting experiments were performed according to ASTM D4843-88 [36]. During the drying process, each sample was placed in an oven with temperature at 60 ± 1°C for 23 h. In the subsequent wetting process, the sample was placed on a porous stone in an immersion chamber with temperature controlled at 20 ± 1°C for 1 h. Distilled water was used to saturate the porous stone and maintained for 23 h. After 1, 3, 5, 7, 10, and 15 cycles of the drying-wetting process, the free swelling ratio, swelling pressure, and the compressibility tests were performed in accordance with ASTM D4546 [37] and ASTM D 2435 [38].

2.3. Swelling Potential Tests. Swelling potential reflects the volume change or the pressure required to prevent swelling [39]. The swelling ratio was adopted to describe the swelling potential, which is defined as the ratio of the swelling amount to the original thickness in percentage. The swelling ratio tests were carried out using a one-dimensional oedometer apparatus. The sample in the ring was placed between two porous stones, and filter papers were added between the sample and the porous stones. A static pressure of 0.7 kPa was applied. The sample was then soaked in water and allowed to swell under initial static pressure. The dial gauge displacement was recorded until no further swelling, where the swelling potential was considered as full completion. Based on the measured results, the free swelling ratio was calculated using the following equation:

$$\delta_N = \frac{\Delta H}{H_0} = \frac{H_N - H_0}{H_0}, \tag{1}$$

where δ_N (%) and H_N (mm) are the free swelling ratio and height of the sample after swelling, respectively, and H_0 (mm) is the initial height.

2.4. Swelling Pressure Tests. The swelling pressure tests were measured using the constant volume method. The sample installed in the 1D oedometer apparatus was the same as the swelling ratio test. The water-soaked sample was subjected to a specific load to keep constant volume. The load was tracked when no further swelling was observed. Swelling pressure was calculated using the following equation:

$$P_e = \frac{W}{A} \times 10, \tag{2}$$

where P_e (kPa) is the swelling pressure, W (N) is the total load, and A (cm^2) is the area of sample.

2.5. Compressibility Tests. The compressibility tests were carried out by using an automatic pneumatic 1D oedometer and computer data acquisition and processing system. The step-step loads (25, 50, 100, 200, 400, and 800 kPa) were applied until 24 hrs. The sample installation in the 1-D oedometer apparatus was the same as the swelling ratio test. The compressibility can be evaluated using the coefficient of compressibility from 100 kPa to 200 kPa of the effective

Table 1: Basic physical properties of the tested soils.

ρ (g/cm^{-3})	Gs	e	Atterberg limits (%)		Plasticity index	δ_{ef} (%)	$\rho_{d\max}$ (g/cm^3)	ω_{op} (%)	Grain-size distribution (%)		
			Liquid limit	Plastic limit					Sand	Silt	Clay
1.93	2.74	0.74	46.40	22.10	24.30	53.00	1.84	16.60	4	68	28

ρ, density; Gs, specific gravity; e, void ratio; δ_{ef}, free swelling ratio; $\rho_{d\max}$, maximum dry density; ω_{op}, optimal water content.

Table 2: Chemical composition of calcium carbide slag.

Material	SiO_2	CaO	MgO	Al_2O_3	Fe_2O_3	SO_3
Content (%)	4.21	68.36	0.27	2.79	0.51	0.19

Table 3: Chemical composition of iron tailing sand.

Material	SiO_2	CaO	MgO	Al_2O_3	Fe_2O_3	SO_3
Content (%)	67.92	3.68	4.79	8.11	10.86	4.64

Table 4: Grain size distribution of iron tailing sand.

Grain size	<2 mm	<1 mm	<0.5 mm	<0.25 mm	<0.075 mm
Content (%)	98.28	97.13	89.98	60.92	7.21

Table 5: Compaction characteristics.

a_{ITS} (%)			30		
a_{CCS} (%)	6	8	10	12	14
Optimum water content (%)	13.2	13.5	13.8	14.2	14.7
Maximum dry density (g/cm^3)	1.895	1.885	1.872	1.859	1.844

vertical stress [40]. The coefficient of compressibility was calculated using the following equation:

$$a_v = \frac{e_1 - e_2}{p_2 - p_1}, \tag{3}$$

where a_v (kPa^{-1}) is the coefficient of compressibility and e_1 and e_2 are the void ratio under P_1 (100 kPa) and P_2 (200 kPa), respectively.

2.6. Scanning Electron Microscopy (SEM) and Mercury Intrusion Porosimetry (MIP). Scanning electron microscopy (SEM) and mercury intrusion porosimetry (MIP) were used to investigate the microstructure and the pore characteristics of the modified soils. In the SEM procedure, the samples were cut into pieces with approximately 1 cm^3, gold coated, and then scanned by using a high-resolution scanning electron microscope. MIP tests were carried out on an automatic mercury intrusion instrument. According to MIP requirement, the samples were cut into small pieces and the lyophilization technique should be first adopted.

3. Results and Discussions

3.1. Swelling Potential and Pressure. The evolutions of the free swelling ratio and swelling pressure with the number of drying-wetting cycles in the present work are shown in Figures 1 and 2, respectively. From these figures, it can be seen that both the free swelling ratio and swelling pressure initially increase and subsequently decrease with the increasing cycles. As shown in Figures 1 and 2, the tendency in swelling potential is the same in clay fraction (Figure 3) when encountering the drying-wetting cycles. The tendency indicates that the clay fraction increases the swelling ratio. After the process of the drying-wetting cycles, this clay existence is probably released from the modified soil aggregates for the partial breakdown and disintegration, in agreement with the observations of previous studies [23, 24]. After the seventh cycle, the maximum values of the swelling ratio and swelling pressure occur. Meanwhile, the maximum value of the free swelling ratio is below 30% (limit line in Figure 1), which satisfies the requirement of backfilling materials in Jianghuai area of Anhui province [40]. The value of swelling pressure with optimal CCS of 10% is below 45 kPa (limit line in Figure 2), which depends on the overburden vertical stress of applied subgrade layer. Note that the free swelling ratio, the swelling pressure, and the clay fraction all decrease after seventh cycles, which is different with the observation of the free swelling ratio and the swelling pressure in the previous studies. This trend may be related to loss of clay fraction or transformation of clay mineral by CCS. The excessive drying-wetting cycles may lead to the serious damage of soil structure and the porosity, and the clay fraction releasing from the aggregates is lost from the pores with the infiltration and flow during the wetting-drying cycles [24].

3.2. Compressibility. The effect of drying-wetting cycles on compressibility is presented in Figure 4. The compressibility can be divided into two stages. In the first stage, the compressibility increases rapidly. In the second stage, the compressibility increases slowly and reaches to a relatively stable state after the tenth drying-wetting cycle. This increase trend is contributed to the irresistible deformation under volumetric stress which caused by the destruction of cementitious products and loose matrix structure. This stable state reveals that the effects of drying-wetting cycles are resisted, which indicates some stronger cementitious compounds after drying-wetting cycles are regenerated. The compressibility evolution is consistent with the results of Stoltz et al. [25]. It is worth noting that the coefficient of compressibility with a_{CCS} of 10% is lower than that of 6%, 8%, 12%, and 14%, suggesting that the structure with a_{CCS} of 10% is more compact than that of 6%, 8%, 12%, and 14%.

With these results, evolution of the compressibility with the drying-wetting cycles can be described using equation (4), with the specific parameters listed in Table 5:

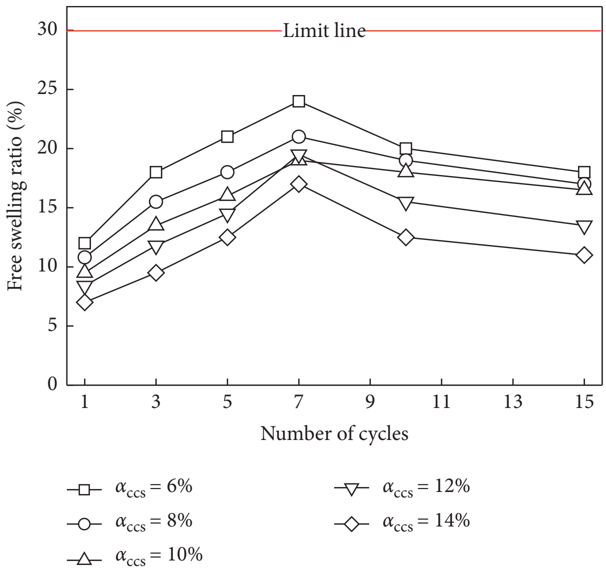

Figure 1: Free swelling ratio during the drying-wetting process.

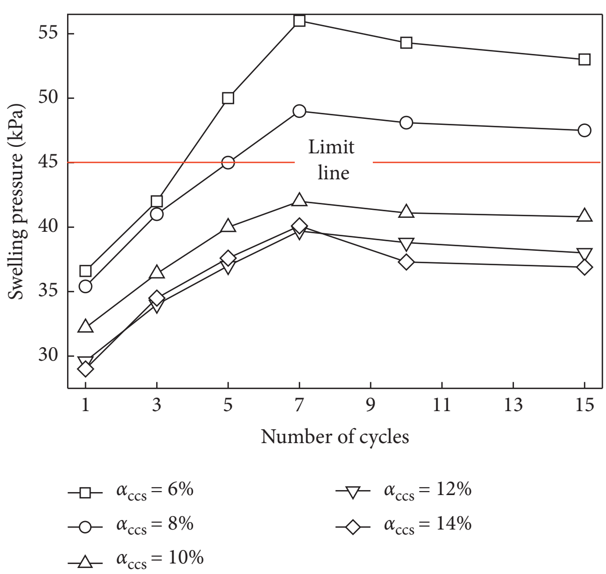

Figure 2: Swelling pressure during the drying-wetting process.

$$\alpha = A \cdot \exp(B \cdot N) + C, \tag{4}$$

where α is the compressibility (MPa^{-1}) and N is the number of drying-wetting cycles.

As shown in Table 6, parameters A, B, and C change very little with a_{CCS}, but dependent on $a_{CCS.}$.

It is clearly shown that the compressibility is strongly related to the cycle numbers, as the parallel curves shown in Figure 5. Therefore, an empirical relationship can be used to predict the compressibility of the expansive soil treated with iron tailing sand and calcium carbide slag experiencing drying-wetting cycles.

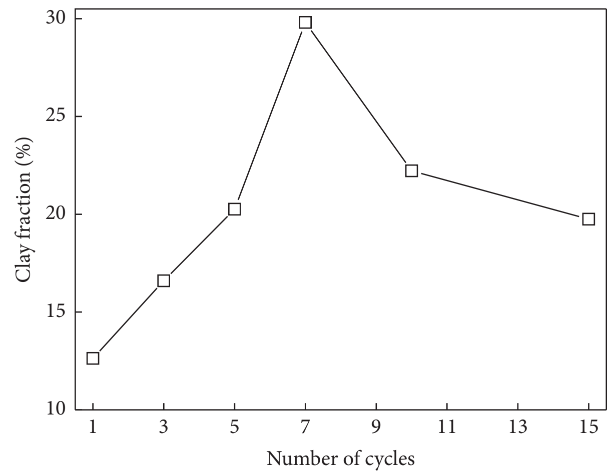

Figure 3: Relationships between the clay fraction and the number of drying-wetting cycles.

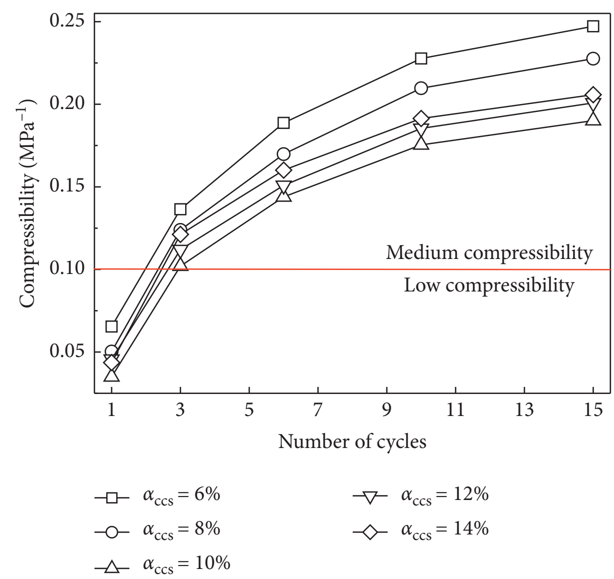

Figure 4: The variation of compressibility during the wetting-drying cycles.

3.3. Microstructure by SEM and MIP. The pore size distribution of mercury intrusion porosimetry tests is presented in Figure 6. From Figure 6(a), the PSD distribution shows the typical bimodal characteristics, indicating the presence of two groups of pores: macropores and micropores. Note that the averages of total volume in macropores and micropores slightly increase with the number of drying-wetting cycles in Figure 6(b). The final intrusion volume keeps increasing during the wetting-drying process, which is also

Table 6: Parameters in determining the coefficient of compressibility.

α_{CCS} (%)	A	B	C	Fitting degree (R^2)
6	−0.23	−0.21	0.26	0.998
8	−0.23	−0.22	0.23	0.994
10	−0.20	−0.25	0.19	0.995
12	−0.20	−0.23	0.21	0.992
14	−0.21	−0.28	0.21	0.988

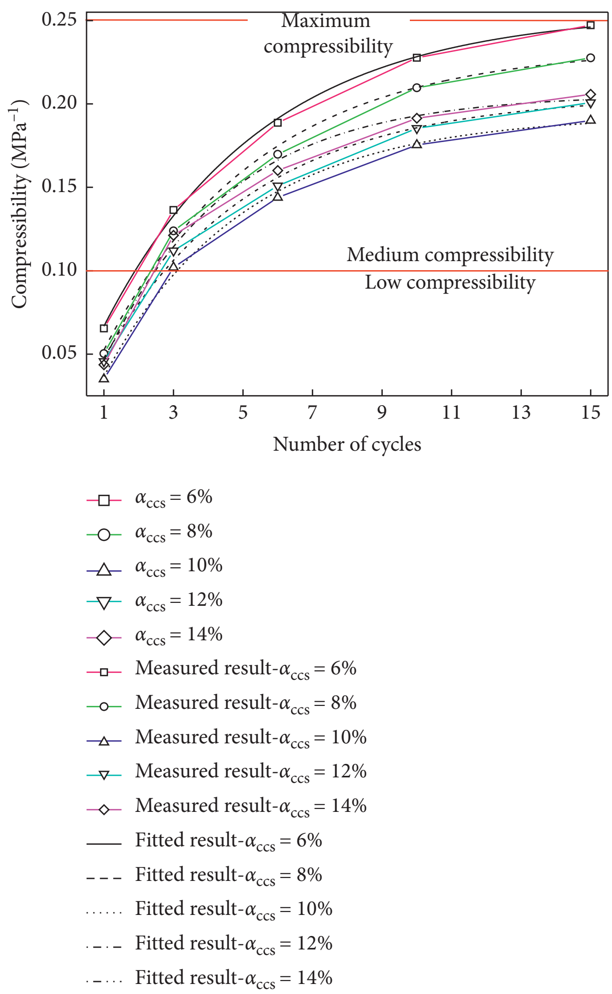

Figure 5: Relationships between the compression coefficient and the number of drying-wetting cycles.

consistent with the tendency of compressibility encountering the drying-wetting cycles.

To differentiate the porosity within the modified soils, the pore group would be classified. Kong et al. [41] divided the pores into micropores (<0.007 μm) within the particles, small pores (0.007 μm~0.9 μm) between the particles, middle pores (0.9 μm~35 μm) within the aggregates, large pores (35 μm~300 μm) between the aggregates, and the macropores (>300 μm). Figure 6 shows the pore sizes subjected to drying-wetting cycles which mainly lie in 0.007~0.9 μm and 0.9~35 μm, suggesting that small and medium pores are majority (more than 85%). Note that the volume of small and middle pores increases from the first cycle to the tenth cycle.

The evolution of stabilized soil during the drying-wetting process is presented from the SEM results in Figure 7. After

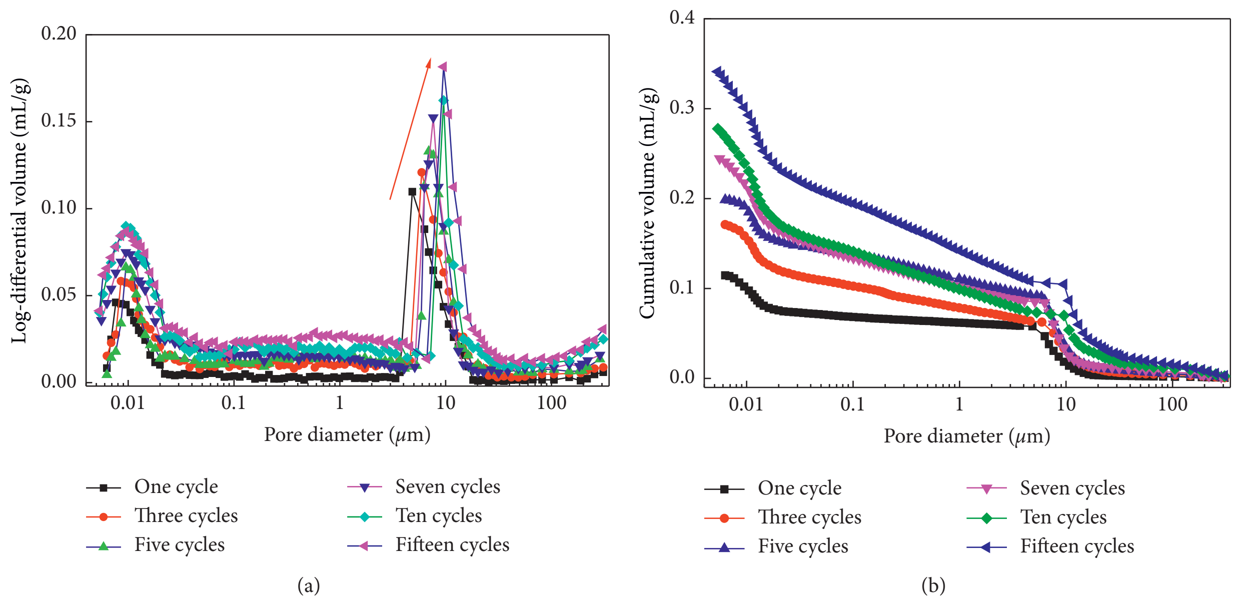

Figure 6: Pore size distribution of improved soils with different numbers of drying-wetting cycles for (a) log-differential distribution and (b) cumulative distribution.

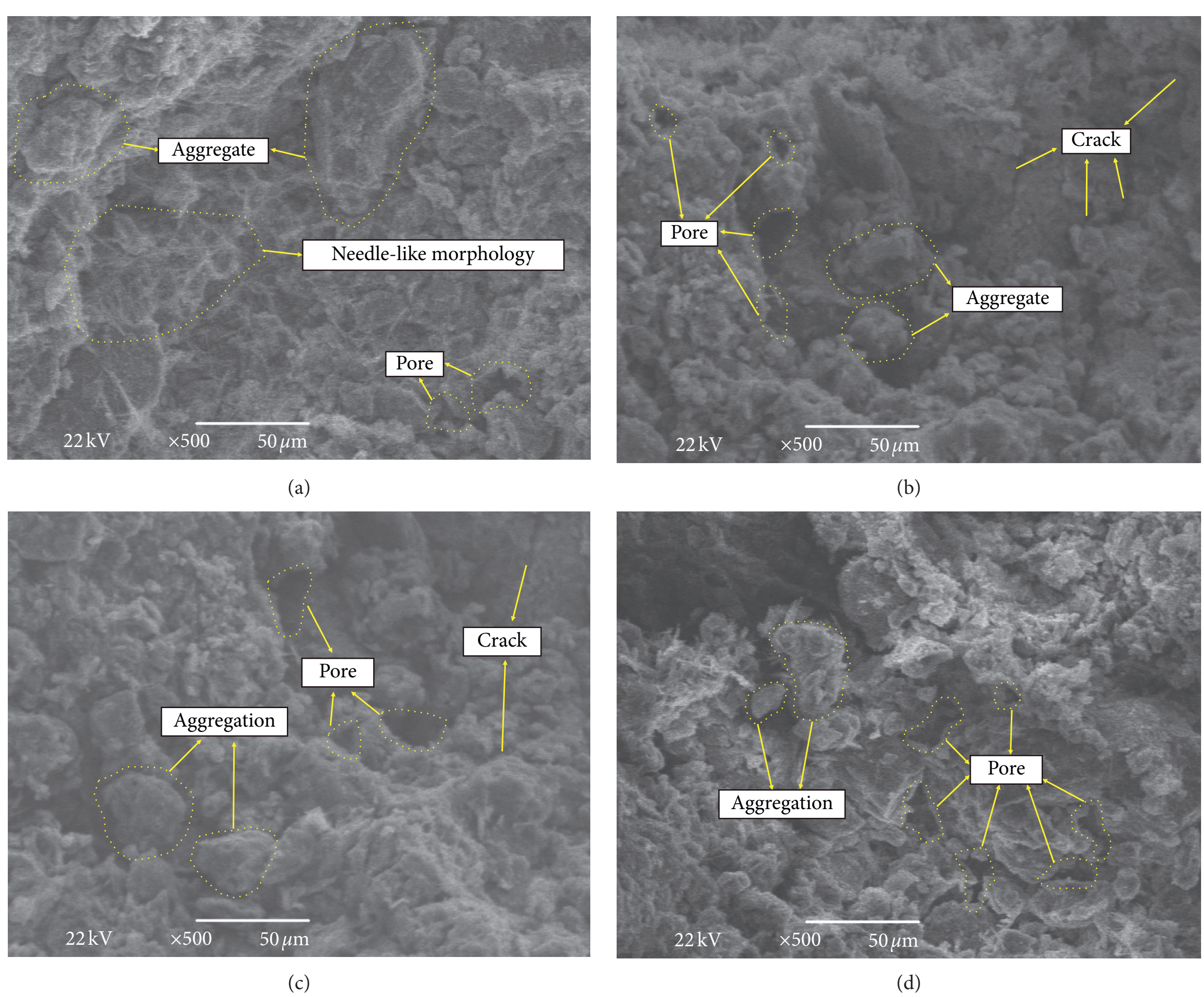

Figure 7: Microstructural feature encountering drying-wetting cycles. (a) 1st cycle, (b) 5th cycle, (c) 7th cycle, and (d) 10th cycle.

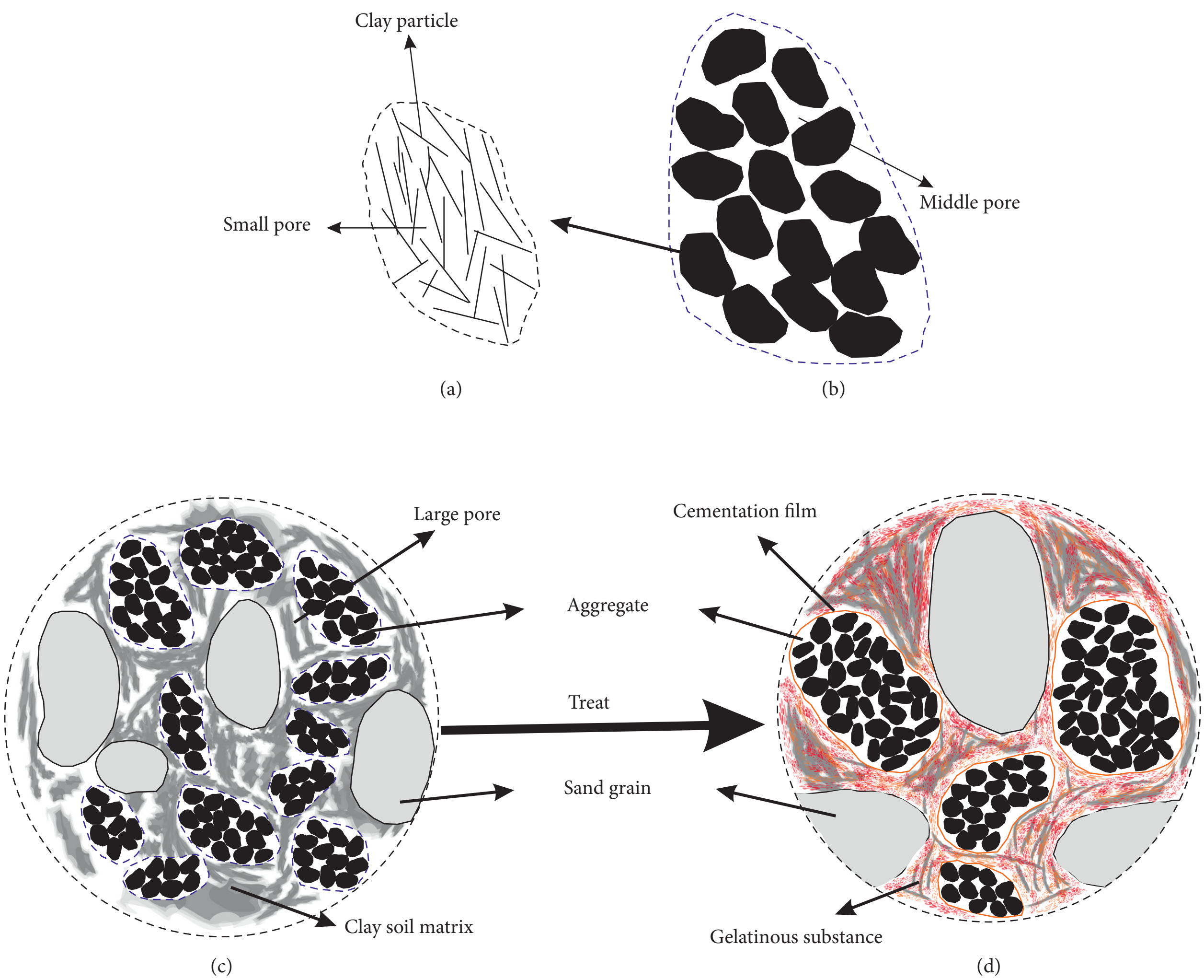

Figure 8: Structure of flocculated fabric (a), aggregate (b), raw soil (c), and improved soil (d).

the first cycle, the microstructure of stabilized soils is compact and contains needle-like morphology. The aggregates are big, and the pores in improved soil are mainly composed of the medium pores. After the fifth cycle, the binding of cementitious compounds and protection of cementation were mostly retained. The small and middle pores changed trivially. After the seventh cycle, the aggregates are severely damaged and become smaller in dimension. The pore volume between aggregates increases significantly. After the tenth cycle, the aggregates become weak and the pores within aggregates increase seriously.

For the compacted soils, the microstructure should involve two structural levels, i.e., among and within aggregates [42–44]. This classification (double porosity) plays an important role in the hydraulic strength and deformation behaviours [45–47]. This model of double porosity [48, 49] was attempted to clarify the structure characteristic of original and stabilized soils in the present work shown in Figure 8. According to analysis by SEM images, the structure among aggregates became looser and that within aggregates is destroyed and dispersed with the increase number of drying-wetting cycles. The disintegration of soluble substances and the effects of swelling and shrinkage lead to the destruction of partial gelatinous substance and the generation of cracks and pores. In view of the skeleton structure, macroaggregates contribute to the limitation of the swelling potential and the swelling pressure more than microaggregates, which suggests that the change in macroaggregates is consistent with that in macroscopic swelling characteristics.

4. Conclusions

The impacts of successive drying-wetting cycles on the swelling properties, the compressibility, and the microstructure of expansive soil improved by iron tailing sand and calcium carbide slag have been investigated in this study. Effects of changes in iron tailing sand and calcium carbide content and curing time were discussed. The main conclusions have been drawn as follows:

(1) The variation of swelling potential and the swelling pressure is closely related to the clay fraction. The swelling behaviour of modified expansive soils subjected to the drying-wetting cycles is a gradual destructive process and can be predicted by the function of the cycle number.

(2) Despite the negative effect of drying-wetting cycles, the iron tailing sand and calcium carbide are effective in stabilizing the expansive soil.

(3) Drying-wetting cycles enrich the porosity within and among the aggregates, suggesting the progressive damage process of the soil structure.

(4) Aggregates play an important role in improving expansive soil. The wetting-drying cycle has an influence on the modified expansive soils in the transformation of the aggregates.

Data Availability

The data used to support the findings of this study are included within the article.

Conflicts of Interest

The authors declare no conflicts of interest.

Acknowledgments

This study was supported by the National Natural Science Foundation of China (Grant nos. 51878159 and 41577280).

References

[1] A. A. Al-Rawas, I. Guba, and A. Mcgown, "Geological and engineering characteristics of expansive soils and rocks in northern Oman," *Engineering Geology*, vol. 50, no. 3-4, pp. 267–281, 1998.

[2] B. Shi, H. Jiang, Z. Liu, and H. Y. Fang, "Engineering geological characteristics of expansive soils in China," *Engineering Geology*, vol. 67, no. 1-2, pp. 63–71, 2002.

[3] S. L. Houston, H. B. Dye, C. E. Zapata, K. D. Walsh, and W. N. Houston, "Study of expansive soils and residential foundations on expansive soils in Arizona," *Journal of Performance of Constructed Facilities*, vol. 25, no. 1, pp. 31–44, 2011.

[4] Y. Liu and S. K. Vanapalli, "Influence of lateral swelling pressure on the geotechnical infrastructure in expansive soils," *Journal of Geotechnical and Geoenvironmental Engineering*, vol. 143, no. 6, Article ID 04017006, 2017.

[5] E. J. Nelson, K. C. Chao, J. D. Nelson, and D. D. Overton, "Lessons learned from foundation and slab failures on expansive soils," *Journal of Performance of Constructed Facilities*, vol. 31, no. 3, Article ID D4016007, 2017.

[6] A. A. Al-Rawas, A. W. Hago, and H. Al-Sarmi, "Effect of lime, cement and sarooj (artificial pozzolan) on the swelling potential of an expansive soil from Oman," *Building and Environment*, vol. 40, no. 5, pp. 681–687, 2005.

[7] T. Kamei, A. Ahmed, and K. Ugai, "Durability of soft clay soil stabilized with recycled bassanite and furnace cement mixtures," *Soils and Foundations*, vol. 53, no. 1, pp. 155–165, 2013.

[8] M. Khemissa and A. Mahamedi, "Cement and lime mixture stabilization of an expansive overconsolidated clay," *Applied Clay Science*, vol. 95, pp. 104–110, 2014.

[9] J. Yang, J. L. Wang, G. D. Zhang, Y. W. Tang, and Z. G. Xie, "Comparative experiment research on different material improvement to the influence of expansive soil expandability," *Advanced Materials Research*, vol. 598, pp. 574–579, 2012.

[10] U. Hasan, A. Chegenizadeh, M. A. Budihardjo, and H. Nikraz, "Experimental evaluation of construction waste and ground granulated blast furnace slag as alternative soil stabilisers," *Geotechnical and Geological Engineering*, vol. 34, no. 6, pp. 1707–1722, 2016.

[11] H. Mujtaba, T. Aziz, K. Farooq, N. Sivakugan, and B. M. Das, "Improvement in engineering properties of expansive soils using ground granulated blast furnace slag," *Journal of the Geological Society of India*, vol. 92, no. 3, pp. 357–362, 2018.

[12] A. Soltani, A. Deng, and A. Taheri, "Swell-compression characteristics of a fiber-reinforced expansive soil," *Geotextiles and Geomembranes*, vol. 46, no. 2, pp. 183–189, 2018.

[13] H. Ye, C. Chu, L. Xu, K. Guo, and D. Li, "Experimental studies on drying-wetting cycle characteristics of expansive soils improved by industrial wastes," *Advances in Civil Engineering*, vol. 2018, Article ID 2321361, 9 pages, 2018.

[14] Y. Yilmaz, "Compaction and strength characteristics of fly ash and fiber amended clayey soil," *Engineering Geology*, vol. 188, pp. 168–177, 2015.

[15] B. Li, Z. Y. Zhao, B. T. Tang, H. B. Li, H. C. Chen, and Z. Ma, "Comprehensive utilization of iron tailings in China," *IOP Conference Series: Earth and Environmental Science*, vol. 199, Article ID 42055, 2018.

[16] S. Zhang, X. Xue, X. Liu et al., "Current situation and comprehensive utilization of iron ore tailing resources," *Journal of Mining Science*, vol. 42, no. 4, pp. 403–408, 2006.

[17] C. Chu, Y. Deng, A. Zhou, Q. Feng, H. Ye, and F. Zha, "Backfilling performance of mixtures of dredged river sediment and iron tailing slag stabilized by calcium carbide slag in mine goaf," *Construction and Building Materials*, vol. 189, pp. 849–856, 2018.

[18] Y. Yi, L. Gu, S. Liu, and A. J. Puppala, "Carbide slag-activated ground granulated blastfurnace slag for soft clay stabilization," *Canadian Geotechnical Journal*, vol. 52, no. 5, pp. 656–663, 2015.

[19] S. B. Ikizler, M. Aytekin, and M. Vekli, "Reductions in swelling pressure of expansive soil stabilized using EPS geofoam and sand," *Geosynthetics International*, vol. 16, no. 3, pp. 216–221, 2009.

[20] L. Yang and X. Deng, "Experimental study on shear behavior of expansive soil modified by gravel sand," *IOP Conference Series: Materials Science and Engineering*, vol. 688, Article ID 033021, 2019.

[21] F. Akcanca and M. Aytekin, "Effect of wetting-drying cycles on swelling behavior of lime stabilized sand-bentonite mixtures," *Environmental Earth Sciences*, vol. 66, no. 1, pp. 67–74, 2012.

[22] A. R. Estabragh, M. R. S. Pereshkafti, B. Parsaei, and A. A. Javadi, "Stabilised expansive soil behaviour during wetting and drying," *International Journal of Pavement Engineering*, vol. 14, no. 4, pp. 418–427, 2013.

[23] Y. Guney, D. Sari, M. Cetin, and M. Tuncan, "Impact of cyclic wetting-drying on swelling behavior of lime-stabilized soil," *Building and Environment*, vol. 42, no. 2, pp. 681–688, 2007.

[24] S. M. Rao, B. V. V. Reddy, and M. Muttharam, "The impact of cyclic wetting and drying on the swelling behaviour of stabilized expansive soils," *Engineering Geology*, vol. 60, no. 1-4, pp. 223–233, 2001.

[25] G. Stoltz, O. Cuisinier, and F. Masrouri, "Weathering of a lime-treated clayey soil by drying and wetting cycles," *Engineering Geology*, vol. 181, pp. 281–289, 2014.

[26] E. Kalkan, "Impact of wetting-drying cycles on swelling behavior of clayey soils modified by silica fume," *Applied Clay Science*, vol. 52, no. 4, pp. 345–352, 2011.

[27] B.-t. Wang, C.-h. Zhang, X.-l. Qiu, E.-y. Ji, and W.-h. Zhang, "Research on wetting-drying cycles' effect on the physical and mechanical properties of expansive soil improved by OTAC-KCl," *Advances in Materials Science and Engineering*, vol. 2015, Article ID 304276, 7 pages, 2015.

[28] F. Yazdandoust and S. S. Yasrobi, "Effect of cyclic wetting and drying on swelling behavior of polymer-stabilized expansive clays," *Applied Clay Science*, vol. 50, no. 4, pp. 461–468, 2010.

[29] C. W. W. Ng, D. B. Akinniyi, C. Zhou, and C. F. Chiu, "Comparisons of weathered lateritic, granitic and volcanic soils: compressibility and shear strength," *Engineering Geology*, vol. 249, pp. 235–240, 2019.

[30] G. Rajasekaran and S. Narasimha Rao, "Compressibility behaviour of lime-treated marine clay," *Ocean Engineering*, vol. 29, no. 5, pp. 545–559, 2002.

[31] S. M. Rao and P. Shivananda, "Compressibility behaviour of lime-stabilized clay," *Geotechnical and Geological Engineering*, vol. 23, no. 3, pp. 309–319, 2005.

[32] D. Wang, H. Wang, and X. Wang, "Compressibility and strength behavior of marine soils solidified with MgO-A green and low carbon binder," *Marine Georesources & Geotechnology*, vol. 35, no. 6, pp. 878–886, 2017.

[33] S. X. Chen, Y. U. Song, L. W. Kong, A. G. Guo, and G. S. Liu, "Study on approach to identification and classification of expansive soils," *Rock and Soil Mechanics*, vol. 26, no. 12, pp. 1895–1900, 2005, (in Chinese).

[34] ASTM D698, *Standard Test Methods for Laboratory Compaction Characteristics of Soil Using Standard Effort*, ASTM International, West Conshohocken, PA, USA, 2012.

[35] ASTM D421-85, *Standard Practice for Dry Preparation of Soil Samples for Particle-Size Analysis and Determination of Soil Constants*, ASTM International, West Conshohocken, PA, USA, 2007.

[36] ASTM D4843-88, *Standard Test Method for Wetting and Drying Test of Solid Wastes*, ASTM International, West Conshohocken, PA, USA, 2016.

[37] ASTM D4546, *Standard Test Methods for One-Dimensional Swell or Collapse of Soils*, ASTM International, West Conshohocken, PA, USA, 2014.

[38] ASTM D2435, *Standard Test Methods for One-Dimensional Consolidation Properties of Soils Using Incremental Loading*, ASTM International, West Conshohocken, PA, USA, 2004.

[39] F.-s. Zha, J.-j. Liu, L. Xu, and K.-r. Cui, "Effect of cyclic drying and wetting on engineering properties of heavy metal contaminated soils solidified/stabilized with fly ash," *Journal of Central South University*, vol. 20, no. 7, pp. 1947–1952, 2013.

[40] JTG C20, *Ministry of Transport of the People's Republic of China:Code for Highway Engineering Geological Investigation*, China Communications Press, Beijing, 2011.

[41] L. R. Kong, H. W. Huang, and D. M. Zhang, "Experiment study on relationship between pore distribution and different stress levels due to consolidation of soft clays," *Chinese Journal of Underground Space and Engineering*, vol. 3, no. 6, pp. 1036–1040, 2007, (in Chinese).

[42] A. Gens and E. E. Alonso, "A framework for the behaviour of unsaturated expansive clays," *Canadian Geotechnical Journal*, vol. 29, no. 6, pp. 1013–1032, 1992.

[43] A. Koliji, L. Vulliet, and L. Laloui, "New basis for the constitutive modelling of aggregated soils," *Acta Geotechnica*, vol. 3, no. 1, pp. 61–69, 2008.

[44] A. Koliji, L. Vulliet, and L. Laloui, "Structural characterization of unsaturated aggregated soil," *Canadian Geotechnical Journal*, vol. 47, no. 3, pp. 297–311, 2010.

[45] H. Al-Dakheeli and R. Bulut, "Interrelationship between elastic deformation and soil-water characteristic curve of expansive soils," *Journal of Geotechnical and Geoenvironmental Engineering*, vol. 145, no. 4, Article ID 04019005, 2019.

[46] A. Koliji, L. Laloui, O. Cusinier, and L. Vulliet, "Suction induced effects on the fabric of a structured soil," *Transport in Porous Media*, vol. 64, no. 2, pp. 261–278, 2006.

[47] E. Romero, A. Gens, and A. Lloret, "Water permeability, water retention and microstructure of unsaturated compacted boom clay," *Engineering Geology*, vol. 54, no. 1-2, pp. 117–127, 1999.

[48] R. Thom, R. Sivakumar, V. Sivakumar, E. J. Murray, and P. Mackinnon, "Pore size distribution of unsaturated compacted kaolin: the initial states and final states following saturation," *Géotechnique*, vol. 57, no. 5, pp. 469–474, 2007.

[49] G. Wang and X. Wei, "Modeling swelling-shrinkage behavior of compacted expansive soils during wetting-drying cycles," *Canadian Geotechnical Journal*, vol. 52, no. 6, pp. 783–794, 2015.